# Journal of Materials Chemistry C

Accepted Manuscript


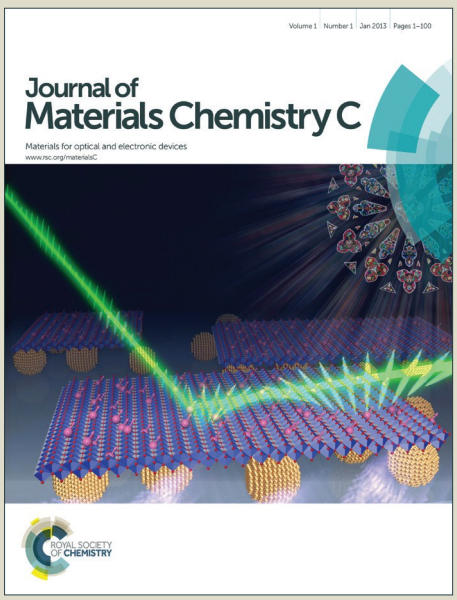





ROYAL SOCIETY OF CHEMISTRY

www.rsc.org/materialsC

Journal Name

RSCPublishing

ARTICLE

# Fast synthesis of Red $Li_3BaSrLn_3(WO_4)_8:Eu^{3+}$ Phosphors for White LED under Near-UV Excitation by Microwave-assisted Solid State Reaction Method and Photo Luminescence Studies

Cite this: DOI: 10.1039/x0xx00000x

Received 00th Oct. 2015,
Accepted 00th Oct. 2015

DOI: 10.1039/x0xx00000x

www.rsc.org/

Bo Wei,*[a,†] Zhenyu Liu,[b,†] Chen Xie,[c] Shu Yang,[a] Wentao Tang,[a] Aiwei Gu,[a] Wing-Tak Wong,*[b] and Ka-Leung Wong*[c]

Red $Li_3BaSrLa_3(WO_4)_8:Eu^{3+}$ phosphors have been successfully synthesized by a rapid microwave-assisted solid state method. The sintered time for the optimal phosphor can be limited to only 10 minutes at 900 ℃. Upon the near-Ultra-Violet (NUV) excitation, strong red emission can be found in 90% $Eu^{3+}$ doped Tungstate compounds. This phosphor exhibits impressive thermal stability, and the purity of red emission $Li_3BaSrLa_3(WO_4)_8:Eu^{3+}$ in high $Eu^{3+}$ doping concentrations can achieve the coordinates values ($x$ = 0.670, $y$ = 0.330), indicating high red color purity. The corresponding quantum yield (QY) is measured (28.36 ±0.09%). Photoluminescence and kinetic studies showed no obvious effects due to concentration quenching effect, cross relaxation and non-radiative energy transfer. The $Li_3BaSrLa_3(WO_4)_8:Eu^{3+}$ can be synthesized with a simple and quick method and the comprehensive photophysical studies of the novel phosphor ($Li_3BaSrLa_3(WO_4)_8:Eu^{3+}$) have been done and the potential as a practical phosphor a for NUV-excited white LEDs (WLEDs) have been shown.

## 1. Introduction

As a promising light source, phosphor converted white light-emitting diodes (pc-WLEDs) have advantages over conventional incandescent and fluorescent materials, such as high energy efficiency, low thermal radiation and long operation time.[1-7] Nowadays, the most widely used WLEDs consist of a 450-470 nm blue InGaN LED chip and $Y_3Al_5O_{12}$: $Ce^{3+}$ (YAG: Ce) yellow phosphor and generate white light by mixing yellow emission from the phosphor and blue light from the chip. However, due to the deficiency of red component this type of WLED suffers from the concerns of high correlated color temperature (>7000K) and low color rendering index (<70).[8-10] Different degradation rates of blue chip and phosphor also result in poor chromaticity coordinates. Consequently, applications of this type of WLEDs on indoor illumination and screen display is limited.[11]

To overcome those drawbacks, there is a trend of blending tricolor (blue, red, green) phosphors and employing them with near ultraviolet chips to avoid degradation of packaging materials.[12] At this moment, commercial red phosphors are mainly nitrides and sulfides. Unfortunately, poor stability of sulfides and difficulty in synthesis of nitrides restrict their applications.[13-16] Therefore, it is necessary and urgent to find a novel oxide-based red phosphor.

Tungstate complexes, a large class of inorganic functional materials have unique physical properties and are applied in the field of optical material.[17-19] Tungstate compounds doped with rare-earth metal ions ($RE^{3+}$) are known as multifunctional materials and extensively applied as laser, scintillator and luminescent materials, because this kind of tungstate complexes, working as self-activating phosphors with good stability and refractive index, endow themselves to have efficient energy transfer from the host to the localized states of the doping ions.[20-23] Many techniques have been employed to prepare the tungstate compounds. For the traditional solid state reaction method, the walls of the reactor are heated up by conduction, and the core of the sample requires longer time to achieve the desired temperature inside the reactor, so it may leads to non-uniformity in temperature profile. Moreover, conventional heating experiments often need long reaction times and consume a large amount of energy.

Microwave heating has been mainly applied to prepare a variety of organic compounds for more than 15 years.[24] Microwaves couple directly with molecules within reaction mixture, leading to a rapid rise in temperature. Various materials have been produced increasingly with the help of microwave energy for example, the preparation of molecular sieve, radiopharmaceuticals, inorganic reactions, and nanocrystalline particles.[25] Microwave synthesis not only has the advantage of short reaction time, but also can achieve narrow size-distribution, higher purity, and better crystallinity, compared with conventional methods.[26-30] At present, high temperature solid state reaction with the assistant of microwave is rarely used, and knowledge in this field is still insufficient. So far, microwave heating as a processing method for the synthesis of tungstate compounds has not been studied.

In this study, red $Li_3BaSrLn_3(WO_4)_8:Eu^{3+}$ phosphors have been successfully synthesized by a rapid microwave-assisted solid state method. The optical property and thermal stability are investigated in detail. Experiments are carried out to find the optimal sintered time, sintered temperature and doping concentration. Besides, quantum yield (QY) is measured and compared with the commercial red phosphors $Y_2O_3:Eu^{3+}$. Moreover, an optical ability comparison of the samples prepared by the microwave-assisted method and traditional method is shown.

## 2. Material and methods

All the chemical reagents used in this experiment are analytical grade without further purification. $Eu_2O_3$ (99.99%), $WO_3$, $SrCO_3$, $BaCO_3$, $La_2O_3$ (99.99%), $Li_2CO_3$ were purchased from Sinopharm Chemical Reagent Co., Ltd. A microwave-assisted high temperature method was used to prepare the powder materials. Stoichiometric starting materials were ground in an agate mortar for a half hour and pre-heated for 20 minutes at 600 ℃ in open crucibles in a microwave muffle furnace (RWS-ML5). Then the products were removed from the furnace after cooled to room temperature, and finely ground with a ball mill (QM-QX04) for at least 3 hours. Finally, the well-ground powder samples were reheated at 900 ℃ for 10 minutes to complete the reaction.

X-ray diffraction (XRD) measurements were performed with a Rigaku diffractometer using Cu Kα X-ray (λ = 1.5406 Å, voltage = 30 kV, and current = 30 mA). Data were recorded with diffraction angle (2θ) ranging from 10° to 80° with 0.02° steps. The spectroscopy characteristics were measured by using a Hitach F-4600 spectrometer. Quantum yields were measured by using a Hitach F-7000 spectrometer and its accessories. Lifetime curves were recorded on a Horiba IBH TemPro using a 355 nm NanoLED as the excitation pulse source.

## 3. Results and discussion

### 3.1 Structural characterization

Figure 1a shows the XRD patterns of $Li_3BaSr(La_{1-x}Eu_x)_3(WO_4)_8$ ($x$ = 0.05, 0.2, 0.4, 0.6, 0.7, 0.8, 0.9, 1), which were all sintered at 900 ℃ for 20 minutes. All the diffraction peaks can be easily indexed to those of the $Li_3Ba_2Gd_3(MoO_4)_8$ (JCPDS No. 77-0830) and they belong to monoclinic with a space group C2/c. No other phase is found indicating that the phase is pure. According to XRD result and comparing with the structures of $Li_3BaSrR_3(WO_4)_8$ (R = La-Lu, Y)[31], $Sr^{2+}$ and $Ba^{2+}$ occupy the same lattice site in $Li_3BaSrLa_3(WO_4)_8$ matrix. As shown in Figure 1b, the diffraction peak shifts toward larger angles gradually with the increasing doping concentrations of $Eu^{3+}$ ions. This was induced by substituting the $La^{3+}$ ions with smaller $Eu^{3+}$ ions and it cause the host lattice to shrink slightly. Comparing to $Sr^{2+}$ (1.26Å) and $Ba^{2+}$ (1.42 Å), the ionic radius of $Eu^{3+}$ ion (1.066Å) is more close to that of $La^{3+}$ ion (1.16 Å), thus the doped $Eu^{3+}$ ions will be more likely to occupy $La^{3+}$ sites.[32] However, the crystalline structure was not affected by the $Eu^{3+}$ doping as shown in the Figure 1(a). The slight shifts of the diffraction peak can explain that the $Eu^{3+}$ ions enter into the host crystals successfully and successively.

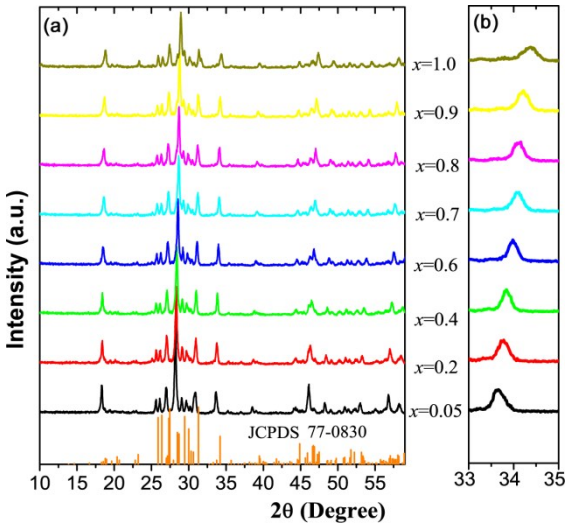


**Fig. 1** (a) XRD spectra of $Li_3BaSr(La_{1-x}Eux)_3(WO_4)_8$ ($x$ = 0.05, 0.2, 0.4, 0.6, 0.7, 0.8, 0.9, 1) sintered at 900 ℃ for 10 minutes. The standard data (JCPDS No. 77-0830) is also presented in the figure for comparison. (b) Shifty toward higher angles of the diffraction peak of the phosphors.

### 3.2 PL excitation and emission spectra

Figure 2 shows the photoluminescence excitation (PLE) spectrum of the $Li_3BaSrLa_3(WO_4)_8$:90%$Eu^{3+}$ phosphors sintered at 900 ℃ for 10 minutes, by monitoring emission at 618 nm ($^5D_0 \rightarrow {}^7F_2$). The spectrum is composed of several narrow excitation peaks originated from the inner *4f-4f* transitions of $Eu^{3+}$ ions and a wider excitation band peaking at 281 nm. This broad band is a charge transfer band attributed to the electron transfer from $O^{2-}$ 2p orbit to $W^{6+}$ 5d orbit inside $WO_4^{2-}$ group, which indicates a wide absorption band in both near-UV and blue regions. The sharp peaks of $Eu^{3+}$ at ~321 nm, ~364 nm, ~383 nm, ~396 nm, ~418 nm, and ~466 nm are corresponded to the transitions of $^7F_J \rightarrow {}^5H_J$, $^7F_0 \rightarrow {}^5D_4$, $^7F_0 \rightarrow {}^5L_7$, $^7F_0 \rightarrow {}^5L_6$, $^7F_0 \rightarrow {}^5L_3$, and $^7F_0 \rightarrow {}^5D_2$, respectively. From the PLE spectrum, we can find two of the most intense peaks located at 396 nm and 466 nm, and both of their intensities are higher than that of the W-O charge transfer band.

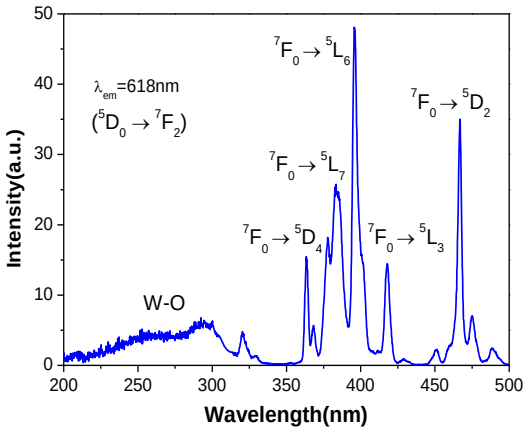


**Fig. 2** The photoluminescence excitation spectrum of the $Li_3BaSrLa_3(WO_4)_8$: 90%$Eu^{3+}$ phosphor sintered at 900 ℃ for 10 minutes, $\lambda_{em}$ = 618 nm ($^5D_0 \rightarrow {}^7F_2$).

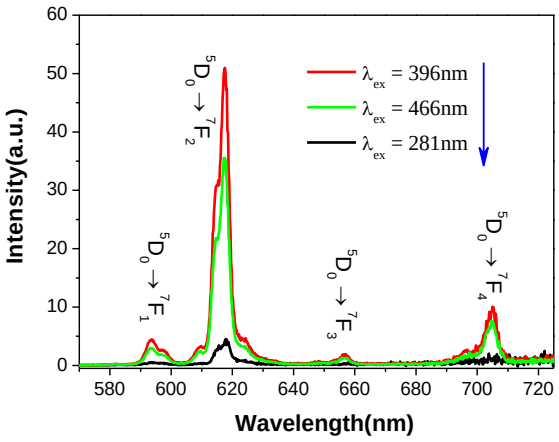


**Fig. 3** Emission spectra of $Li_3BaSrLa_3(WO_4)_8$:90%$Eu^{3+}$ phosphor sintered at 900 ℃ for 10 minutes, $\lambda_{ex}$ = 396 nm, 466nm and 281 nm, respectively.

The emission spectrum of $Li_3BaSrLa_3(WO_4)_8$:90%$Eu^{3+}$ is measured in the range of 570-700 nm under 281 nm excitation in Figure 3. It includes four narrow $^5D_0 \rightarrow {}^7F_J$ (J = 1, 2, 3, 4) emission bands appearing at 587 nm, 618 nm, 622 nm, and 705 nm, respectively. $Eu^{3+}$ ions act as a good probe for the chemical environment of the rare-earth ions because $^5D_0 \rightarrow {}^7F_2$ transition (allowed by forced electric dipole) is very sensitive to the surroundings, while the $^5D_0 \rightarrow {}^7F_1$ transition (allowed by magnetic dipole) is not. In an inversion symmetrical site, the $^5D_0 \rightarrow {}^7F_1$ transition dominates, and when in a site without inversion symmetry, the $^5D_0 \rightarrow {}^7F_2$ transition dominates. From Figure 3 we can see that the 618 nm emission ($^5D_0 \rightarrow {}^7F_2$) is far more intense than 587 nm emission ($^5D_0 \rightarrow {}^7F_1$), indicating that transitions from parity forbidden electric dipole dominate, rather than transitions from magnetic dipole. Most of $Eu^{3+}$ ions occupied the sites without inversion symmetry, which help red emitting phosphors with better performance. We also

showed the emission spectra under excitation of 396 nm and 466 nm in the same figure. Their emission ($^5D_0 \rightarrow {}^7F_{1,2,3,4}$) is more intense than that of 281 nm, which are consistent with the results of PLE spectrum. These observations shown that the $Li_3BaSrLa_3(WO_4)_8:Eu^{3+}$ could be a promising red phosphor for WLEDs under NUV excitation.

### 3.3 Optimal reaction conditions

Figure 4a shows the emission spectra of samples which were synthesized with several sintered temperatures (700 ℃ - 1000 ℃). The emission intensity enhanced with the change in (increasing) sintered temperatures (up to 900 ℃). The Eu emission intensity is diminished after increasing the sintered temperature after 900 ℃. The best sintered temperature is 900 ℃. In Figure 4b, the variate is the sintered time, 10 mins is the optimal sintered time as the highest emission intensity was found.

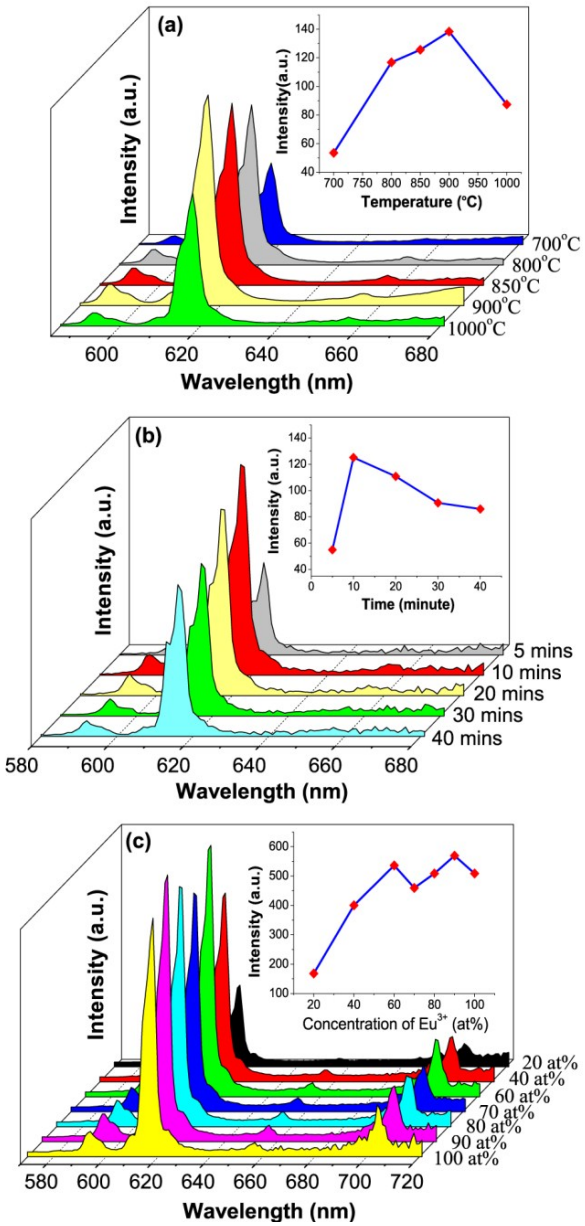


**Fig. 4** (a) Emission spectra of $Li_3BaSr(La_{1-x}Eu_x)_3(WO_4)_8$:5%$Eu^{3+}$ at different sintered temperatures. Inset: Emission intensities of samples variation with temperatures. (b) Emission spectra of $Li_3BaSr(La_{1-x}Eu_x)_3(WO_4)_8$:5%$Eu^{3+}$ in different sintered times at 900 ℃. Inset: Emission intensities of samples variation with sintered times. (c) Emission spectra of $Li_3BaSr(La_{1-x}Eu_x)_3(WO_4)_8$ ($x$ = 0.2, 0.4, 0.6, 0.7, 0.8, 0.9 , 1) sintered for 10 minutes at 900 ℃. Inset: Emission intensities of samples variation with $Eu^{3+}$ ions doping concentration ($\lambda_{ex}$ = 396 nm).

Figure 4c shows the emission spectra of $Li_3BaSr(La_{1-x}Eu_x)_3(WO_4)_8$ ($x$ = 0.2, 0.4, 0.6, 0.7, 0.8, 0.9 , 1) sintered for 10 minutes at 900 ℃. With increasing doping concentrations of $Eu^{3+}$ ions, spectra profiles and peak positions were almost unchanged. The intensities of the major emission, 618 nm from $Eu^{3+}$: $^5D_0 \rightarrow {}^7F_2$ transition, increase with the increase of the doping concentration. The emission intensity ($^5D_0 \rightarrow {}^7F_J$) enhanced dramatically with the $Eu^{3+}$ doped concentrated at 60%. The enhancement increased slowly when the doped concentration larger than 60%. The intensity curve shown in the inset figure 4c, the highest emission intensity occurred at 90 at% $Eu^{3+}$ doping. As the activator ion, $Eu^{3+}$ is the luminescent center of the host material $Li_3BaSrLa_3(WO_4)_8$ with substituting $La^{3+}$ ions. $Eu^{3+}$ ions can accept energy both from host charge transfer band and upper energy levels of itself under blue light excitation. Naturally, the emission intensity will be enhanced as the concentration of doping activator ions increases. However, with continually increasing doping amounts, the distance between activator ions will be shorter and defects originated from lattice mismatch will be increased, leading to concentration quenching from cross relaxation and non-radiative energy transfer, respectively. For the emission intensities, competitions between increasing activator concentrations and energy quenching occur when doping concentration is larger than 60 at% and in consequence a vacillation change is observed.

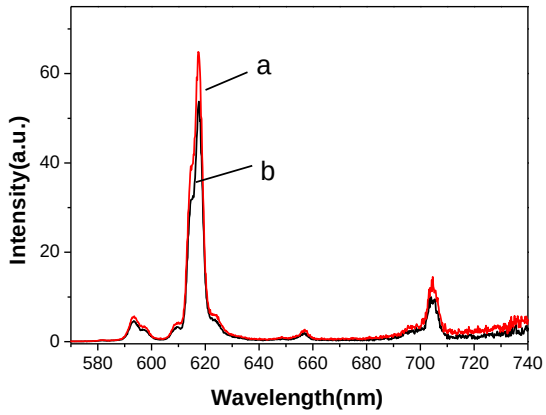


**Fig. 5** Emission spectra of $Li_3BaSrLa_3(WO_4)_8$:90at%$Eu^{3+}$ under 396 nm excitation. (a) Prepared by microwave-assisted solid state method and (b) prepared by traditional high temperature solid state method.

To compare the optical properties of our samples prepared with the microwave-assisted method, we synthesized the same "new sample" (with microwave-assisted method) and "old sample" (with traditional method) respectively. The optical luminescence spectra are shown in Fig. 5, which shows that the main emission peak of the new sample is a little higher than that of the old sample. As mentioned in last section, the optimal sintered time for our samples via the microwave-assisted method is only 10 minutes, which is much shorter than the traditional method, while optical performance is still slightly better compared with the one from conventional synthesizing method, indicating that the microwave-assisted solid state reaction process is an improved and faster method.

### 3.4 Thermal properties of phosphors

The thermal stability of phosphor is one of the important technological parameters for evaluating a phosphor to be applied as WLED.[4] The temperature dependence from 30 ℃ to 230 ℃ of $Li_3BaSrLa_3(WO_4)_8:Eu^{3+}$ emission intensity curves are shown in Fig. 6. It can be seen that with increasing temperature, the emission intensities gradually decrease. Generally, the PL intensity of phosphors at 150℃ with respect to that at room temperature is used to access the thermal stability.[33] A decay of 22% for the phosphor at 130 ℃ (403 K) is observed, indicating that the phosphor has relatively good thermal stability against the thermal quenching effect. The thermal quenching mechanism can be well explained by using a configurational coordinate diagram and the thermal quenching is caused by thermally activated crossover from the excited state to the ground state.[34]

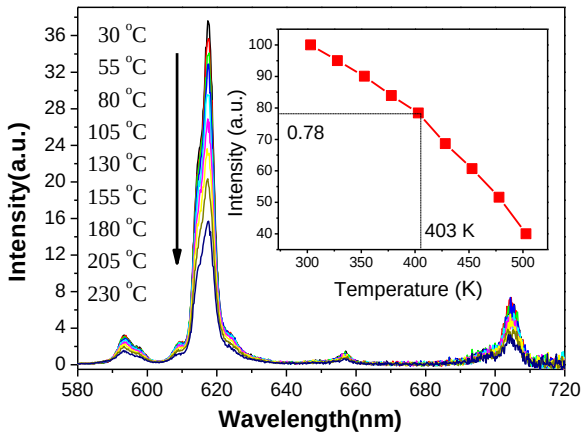


**Fig. 6** Temperature dependence of $Li_3BaSrLa_3(WO_4)_8$: 90at%$Eu^{3+}$ photo luminescence properties under 396 nm excitation.

### 3.5 Chromaticity coordinates of phosphors and quantum yield

From the PL spectra upon excitation at 396 nm, the *x* and *y* values of the Commission Internationale L'Eclairage (CIE), chromaticity coordinates for the $Li_3BaSrLa_3(WO_4)_8$: *x* at% $Eu^{3+}$ (*x* = 90) sample can be determined (Figure 7). Furthermore, chromaticity coordinates of $Li_3BaSrLa_3(WO_4)_8$: *x* at% $Eu^{3+}$ (*x* = 20, 40, 60, 70, 80, 90, 100) are listed in Table 1. From the table, it can be seen that the coordinates of phosphors with higher $Eu^{3+}$ doping concentrations exhibit values very close to the standard coordinates (*x* = 0.670, *y* = 0.330) from NTSC (National Television Standards Committee), indicating a purity of our phosphors. With the increasing $Eu^{3+}$ content, the CIE coordinates of the samples have no obvious change, while the optimal composition for the realization of red light is the one with 90% $Eu^{3+}$ doping, which is consistent with the synthesis result.

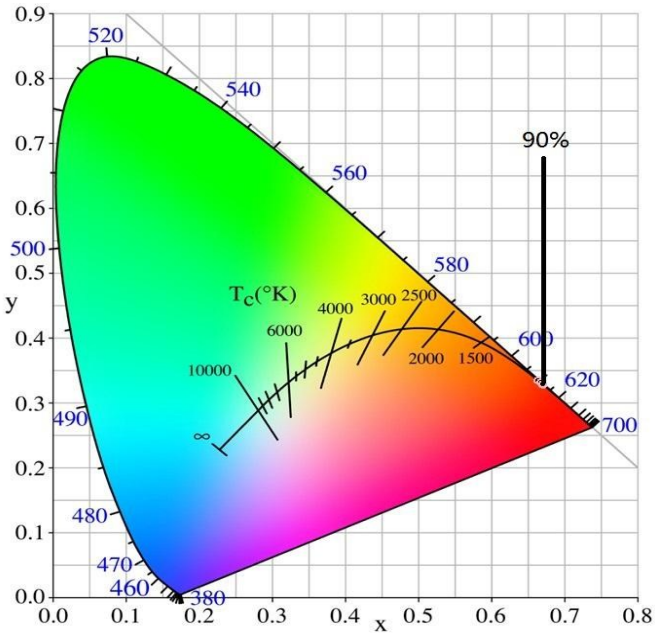


**Fig. 7** Representation of the CIE chromaticity coordinates of $Li_3BaSrLa_3(WO_4)_8$: *x* at% $Eu^{3+}$: (*x* = 90).

**Table 1** Calculated chromaticity coordinates of $Li_3BaSrLa_3(WO_4)_8$: *x* at% $Eu^{3+}$ (*x* = 20, 40, 60, 70, 80, 90, 100) under excitation of 396 nm.

| No. | Doping concentrations | CIE | |
|---|---|---|---|
| | | ***x*** | ***y*** |
| 1 | 20%Eu | 0.6635 | 0.3352 |
| 2 | 40%Eu | 0.6691 | 0.3302 |
| 3 | 60%Eu | 0.6678 | 0.3316 |
| 4 | 70%Eu | 0.6701 | 0.3293 |
| 5 | 80%Eu | 0.6704 | 0.3291 |
| 6 | 90%Eu | 0.6709 | 0.3285 |
| 7 | 100%Eu | 0.67 | 0.3293 |
| | Standard Values | 0.67 | 0.33 |

The corresponding QY of $Li_3BaSrLa_3(WO_4)_8$:90at%$Eu^{3+}$ is found as 28.36±0.09%. The QY of $Y_2O_3$:$Eu^{3+}$ can be 90% under excitation of ~270 nm. However QY is only ~9.6% with the excitation at 396 nm.[19] The QY of our sample is three times higher than the commercial $Y_2O_3$:$Eu^{3+}$ with the excitation at 396 nm.

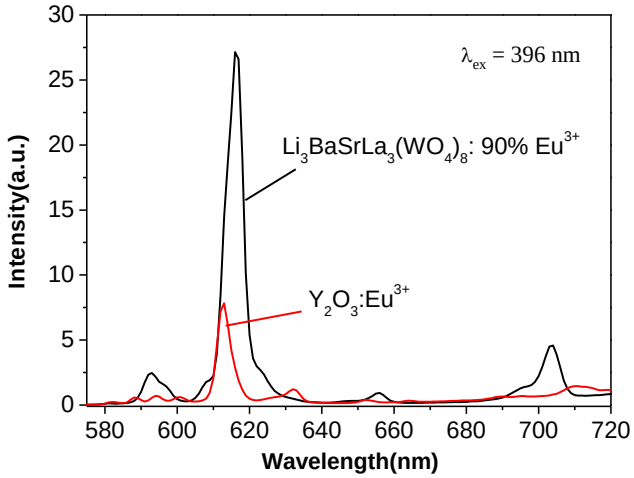


**Fig. 8** Emission spectra comparison between $Li_3BaSrLa_3(WO_4)_8$:90at%$Eu^{3+}$ and the commercial $Y_2O_3$:$Eu^{3+}$ phosphor under 396 nm excitation.

We also measured the lifetimes of our samples (not shown) and their values (~540 - ~580 μs) have no obvious change under 355 nm excitation. For the samples doped with $Eu^{3+}$ ions (from 20% to 100%), their emission intensities are similar according to Figure 4c, thus the kinetic result is consistent with the emission spectra. In view of our results indicate that the concentration quenching effect, the cross relaxation and non-radiative energy transfer are inconspicuous, further showing the good optical property of our materials.

## 4. Conclusion

In conclusion, we have synthesized a red $Li_3BaSrLa_3(WO_4)_8$: 90at%$Eu^{3+}$ phosphor by a new and rapid microwave-assisted solid state method. 10 minutes and 900 ℃ are the optimal sintered time and temperature for synthesizing the $Li_3BaSrLa_3(WO_4)_8$:90at%$Eu^{3+}$ phosphor. Comprehensive photophysical studies have been done to confirm the red emission which is from the $^5D_0 \rightarrow {}^7F_2$transition of europium in $Li_3BaSrLa_3(WO_4)_8$:90at%$Eu^{3+}$ phosphor. Compared with different $Eu^{3+}$ doped concentration in $Li_3BaSrLa_3(WO_4)_8$:90at%$Eu^{3+}$ doping concentration shown the highest emission with 28.36±0.09% quantum yield. The $Li_3BaSrLa_3(WO_4)_8$:90at%$Eu^{3+}$ phosphor also exhibited impressive thermal stability and high purity of red emission with coordinates values (*x* = 0.670, *y* = 0.330) from NTSC. The concentration quenching effect, the cross relaxation and non-radiative energy transfer cannot be found in our synthesized $Li_3BaSrLa_3(WO_4)_8$: 90at%$Eu^{3+}$ phosphor. This should be the reason for the impressive red

emission of $Li_3BaSrLa_3(WO_4)_8$:90at%$Eu^{3+}$ phosphor. Our new synthesized $Li_3BaSrLa_3(WO_4)_8$:90at%$Eu^{3+}$ phosphor has potential as a promising materials for NUV-excited WLEDs.

## Author Contributions

†These authors contributed equally.

## Acknowledgements

This work was supported by the HKBU and HKPolyU Joint Research Programme (RC-ICRS/15-16/02F-WKL), Natural Science Foundation of Jiangsu Province (Grant No. BK2012210), the Natural Science Foundation of the Jiangsu Higher Education Institutions of China (Grant No. 10KJB430001) and the Opening Fund of Jiangsu Key Laboratory of Advanced Functional Materials (Grant No. 12KFJJ010).

## Notes and references

[a] *School of Chemistry and Materials Engineering, Jiangsu key Laboratory of Advanced Functional Materials, Changshu Institute of Technology, Changshu, Jiangsu 215500, People's Republic of China, Email: weibo@cslg.cn*
[b] *Department of Applied Biology and Chemical Technology, The Hong Kong Polytechnic University, Hung Hom, Hong Kong SAR, People's Republic of China, Email: wing-tak.wong@polyu.edu.hk*
[c] *Department of Chemistry, Hong Kong Baptist University, Kowloon Tong, Hong Kong SAR, People's Republic of China, Email:klwong@hkbu.edu.hk*

1. C. C. Lin and R.-S. Liu, *J. Phys. Chem. Lett.*, 2011, **2**, 1268-1277.
2. S. Ye, F. Xiao, Y. Pan, Y. Ma and Q. Zhang, *Mat. Sci. Eng: R.*, 2010, **71**, 1-34.
3. G. Wang, X. Gong, Y. Chen, J. Huang, Y. Lin, Z. Luo and Y. Huang, *Opt. Mater.*, 2014, **36**, 1255-1259.
4. M. Xin, D. Tu, H. Zhu, W. Luo, Z. Liu, P. Huang, R. Li, Y. Cao and X. Chen, *J. Mater. Chem. C*, 2015, **3**, 7286-7293.
5. W.-S. Lo, W.-M. Kwok, G.-L. Law, C.-T. Yeung, C. T.-L. Chan, H.-L. Yeung, H.-K. Kong, C.-H. Chen, M. B. Murphy and K.-L. Wong, *Inorg. Chem.*, 2011, **50**, 5309-5311.
6. J. Zou, H. Wu, C. S. Lam, C. Wang, J. Zhu, C. Zhong, S. Hu, C. L. Ho, G. J. Zhou and H. Wu, *Adv. Mater.*, 2011, **23**, 2976-2980.
7. L. Ying, C. L. Ho, H. Wu, Y. Cao and W. Y. Wong, *Adv. Mater.*, 2014, **26**, 2459-2473.
8. Y. Liu, X. Zhang, Z. Hao, X. Wang and J. Zhang, *Chem. Commun.*, 2011, **47**, 10677-10679.
9. Y. Jia, Y. Huang, Y. Zheng, N. Guo, H. Qiao, Q. Zhao, W. Lv and H. You, *J. Mater. Chem.*, 2012, **22**, 15146-15152.
10. J. Li, J.-G. Li, S. Liu, X. Li, X. Sun and Y. Sakka, *J. Mater. Chem. C*, 2013, **1**, 7614-7622.
11. X. Piao, T. Horikawa, H. Hanzawa and K.-i. Machida, *Appl. Phys. Lett.*, 2006, **88**, 161908-161908.
12. M. Jiao, Y. Jia, W. Lü, W. Lv, Q. Zhao, B. Shao and H. You, *J. Mater. Chem. C*, 2014, **2**, 90-97.
13. S. Jones, D. Kumar, R. K. Singh and P. Holloway, *Appl. Phys. Lett.*, 1997, **71**.
14. C. Guo, B. Chu and Q. Su, *Appl. Surf. Sci.*, 2004, **225**, 198-203.
15. R.-J. Xie, N. Hirosaki, Y. Li and T. Takeda, *Materials*, 2010, **3**, 3777-3793.
16. X. Yin, Y. Wang, D. Wan, F. Huang and J. Yao, *Opt. Mater.*, 2012, **34**, 1353-1356.
17. Q. Dai, H. Song, X. Bai, G. Pan, S. Lu, T. Wang, X. Ren and H. Zhao, *J. Phys. Chem. C*, 2007, **111**, 7586-7592.
18. F. Lei and B. Yan, *J. Phys.Chem. C*, 2008, **113**, 1074-1082.
19. S. Long, J. Hou, G. Zhang, F. Huang and Y. Zeng, *Ceram. Int.*, 2013, **39**, 6013-6017.
20. Y. Zhang, N. Holzwarth and R. Williams, *Phys. Rev. B*, 1998, **57**, 12738.
21. G. Cao, X. Song, H. Yu, C. Fan, Z. Yin and S. Sun, *Mater. Res. Bull.*, 2006, **41**, 232-236.
22. E. Tomaszewicz, *Solid State Sci.*, 2006, **8**, 508-512.
23. Y. Su, L. Li and G. Li, *Chem. Mater.*, 2008, **20**, 6060-6067.
24. M. Komorowska-Durka, G. Dimitrakis, D. Bogdał, A. I. Stankiewicz and G. D. Stefanidis, *Chem. Eng. J.*, 2015, **264**, 633-644.
25. K. V. Srinivasan, P. K. Chaskar, S. N. Dighe, D. S. Rane, P. V. Khade and K. S. Jain, *Heterocycles*, 2011, **83**, 2451-2488.
26. X.-H. Liao, N.-Y. Chen, S. Xu, S.-B. Yang and J.-J. Zhu, *J. Cryst. Growth*, 2003, **252**, 593-598.
27. I. Ganesh, B. Srinivas, R. Johnson, B. P. Saha and Y. R. Mahajan, *J. Eur. Ceram. Soc.*, 2004, **24**, 201-207.
28. J. M. Cao, J. Feng, S. G. Deng, X. Chang, J. Wang, J. S. Liu, P. Lu, H. X. Lu, M. B. Zheng, F. Zhang and J. Tao, *J. Mater. Sci.*, 2005, **40**, 6311-6313.
29. B. N. Rao, P. Muralidharan, P. R. Kumar, M. Venkateswarlu and N. Satyanarayana, *Int. J. Electrochem. Sci*, 2014, **9**, 1207-1220.
30. R. F. Gonçalves, A. R. F. Lima, M. J. Godinho, A. P. Moura, J. Espinosa, E. Longo and A. P. A. Marques, *Ceram. Int.*, 2015, DOI: 10.1016/j.ceramint.2015.06.121.
31. N. Kozhevnikova and O. Kopylova, *Russ. J. Appl. Chem.*, 2011, **84**, 1498-1501.
32. R. t. Shannon, *Acta Cryst.*, 1976, **A32**, 751-767.
33. H. Zhu, C. C. Lin, W. Luo, S. Shu, Z. Liu, Y. Liu, J. Kong, E. Ma, Y. Cao, R.-S. Liu and X. Chen, *Nat. Commun.*, 2014, **5**, 4312.
34. P. Dorenbos, *J. Phys.: Condens. Matter*, 2005, **17**, 8103-8111.

## Graphic Abstract

Highly efficient red $Li_3BaSrLa_3(WO_4)_8$:90at%$Eu^{3+}$ phosphor has been synthesized for NUV-excited WLEDs with impressive thermal stability and high purity emission.